THESIS FOR THE DEGREE OF LICENTIATE OF ENGINEERING

Titania supported vanadium oxide catalysts in the NH_3-SCR reaction: Effect of vanadium loading, promoters and aging

Alexander Nellessen

Department of Chemistry and Chemical Engineering
CHALMERS UNIVERSITY OF TECHNOLOGY

Göteborg, Sweden 2023

Titania supported vanadium oxide catalysts in the NH_3-SCR reaction: Effect of vanadium loading, promoters and aging
ALEXANDER NELLESSEN

© ALEXANDER NELLESSEN, 2023

Licentiatuppsatser vid institutionen för kemi och kemiteknik
Chalmers tekniska högskola
Nr 2023:09

Department of Chemistry and Chemical Engineering
Chalmers University of Technology
SE-412 96 Göteborg
Sweden
Telephone: +46 (0)767084885

Printed by Chalmers Reproservice
Göteborg, Sweden 2023

Titania supported vanadium oxide catalysts in the NH_3-SCR reaction: Effect of vanadium loading, promoters and aging
Thesis for the degree of Licentiate of Engineering
ALEXANDER NELLESSEN

Department of Chemistry and Chemical Engineering
Chalmers University of Technology

Abstract

Emissions of nitrogen oxides (NO_x) from combustion processes in mobile sources attract significant attention due to their role as a major source of atmospheric contamination, along with health risks and environmental issues. Since combustion processes in heavy-duty vehicles are expected to be used for a foreseeable future, many efforts have been invested in a suitable deNO_x technology. The selective catalytic reduction with ammonia (NH_3-SCR) over vanadium-based catalysts is one of the most established technologies to control NO_x emissions due to their various benefits. However, the application in mobile sources cause several challenges, as the catalyst has to work under dynamic conditions in a broad temperature window. Promising solutions have emerged with the implementation of promoters to the active vanadium phase.

The rational design for innovative V-based catalysts requires an improved fundamental understanding of the functions and interactions between the included components that affect the catalysts properties. In this work, the effect of the vanadium loading and the implementation of two promoters (Ce, Nb) were investigated. As in automotive applications the thermal deactivation is a challenge, a special focus was set on the aging impact. The results showed that a high vanadium loading favours the low-temperature activity while thermal stability is achieved with a low vanadium loading. The implementation of Ce results in an improved low-temperature activity, while the incorporation of Nb contributes to a higher thermal stability. Infrared spectroscopic methods such as Raman and *in situ* DRIFTS allowed the identification of surface vanadium oxide species and band assignments for the surface hydroxyl groups and adsorbed surface species of the reactants (NH_3, NO). The deconvolution of the NO_x adsorption spectra enabled a comparison of the surface species ratio among the samples.

Keywords: NH_3-SCR, vanadium oxide, VO_x, aging, Nb, Ce, infrared spectroscopy

List of Publications

This thesis is based on the following appended papers:

Paper I:
Impact of vanadium loading and thermal aging on surface properties of titania supported vanadium oxide NH_3-SCR catalysts
Alexander Nellessen, Andreas Schaefer, Anna Martinelli, Agnes Raj, Andrew Newman and Per-Anders Carlsson
Submitted

Paper II:
Study on surface properties of cerium and niobium promoted titania supported vanadium oxide NH_3-SCR catalysts
Alexander Nellessen, Andreas Schaefer, Anna Martinelli, Roberta Villamaina, Agnes Raj, Andrew Newman and Per-Anders Carlsson
Manuscript

My Contribution

Paper I:
I planned and performed the experiments, analyzed the data expect for sample preparation, activity and XPS measurements. I interpreted the results and wrote the first draft of the manuscript, which was finalized together with my co-authors.

Paper II:
I planned and performed the experiments, analyzed the data expect for sample preparation and activity measurements. I interpreted the results together with my co-authors and wrote the first draft of the manuscript.

List of Figures

1.1 NO_x emissions divided by source sector and historical Euro emission standards for heavy-duty vehicles 1

2.1 Proposed vanadium oxide species on the catalyst surface 4
2.2 Standard SCR mechanism 5
2.3 Temperature operating window of a VO_x/TiO_2 catalyst 6

3.1 Schematic representation of Bragg's law 12
3.2 Example of an IR spectrum during NH_3 adsorption 13
3.3 Vibrational modes of isolated ammonia 13
3.4 Schematic illustration of a in situ DRIFTS setup 14

4.1 NO_x conversion on the VO_x/TiO_2 catalysts 18
4.2 SSA and NH_3 uptake of the VO_x catalysts and TiO_2 19
4.3 NO_x conversion, SSA and NH_3 uptake of the promoted VO_x/TiO_2 catalysts 20
4.4 Raman spectra of the VO_x catalysts and TiO_2 21
4.5 DRIFT NH_3 adsorption spectra of the VO_x catalysts and TiO_2 22
4.6 DRIFT NO adsorption spectra of the VO_x catalysts and TiO_2 24
4.7 Relative ratio of NO_x species on the samples 25

Notation

BET	Brunauer-Emmett-Teller
DRIFTS	Diffuse reflectance infrared Fourier transform spectroscopy
NO_x	Nitrogen oxides
SCR	Selective catalytic reduction
SSA	Specific surface area
TPD	Temperature programmed desorption
VO_x	Vanadium oxide
XPS	X-ray photoelectron spectroscopy
XRD	X-ray diffraction

Contents

Abstract iii

List of Publications v

List of Figures vii

Notation ix

Contents xi

1 Introduction 1
1.1 Objectives 2

2 Background 3
2.1 Selective catalytic reduction with ammonia 3
2.2 Vanadium-based SCR catalysts 4
2.2.1 Reaction mechanism and surface ammonia species 5
2.3 Challenges for V-based catalysts in mobile sources 6
2.4 Implementation of promoters 7

3 Methodology 9
3.1 Sample preparation 9
3.2 Catalytic tests 10
3.3 Characterization 10
3.3.1 Nitrogen physisorption 10
3.3.2 Temperature programmed desorption of ammonia 11
3.3.3 Powder X-ray diffraction 11
3.4 Spectroscopic techniques 12
3.4.1 In situ Diffuse Reflectance Infrared Fourier Transform Spectroscopy 14
3.4.2 Peak profiles and deconvolution 15
3.4.3 Raman spectroscopy 15
3.4.4 X-ray photoelectron spectroscopy 16

4 Results and Discussion 17
4.1 Catalytic activity and correlation with physicochemical properties 18
4.1.1 Effect of vanadium loading 18

4.1.2 Effect of promoters 19
4.2 Spectroscopic investigation of the catalyst surface 20

5 Conclusions and Future Work **27**

Acknowledgements **29**

References **31**

1 Introduction

The increased awareness of health and environmental issues caused by exhaust gases from combustion engines has become a matter of public interest over the recent decades. Due to the rising problematics with smog in cities and metropolitan areas, government agencies across the world have introduced emission regulations for particulate matter, carbon monoxide, hydrocarbons and nitrogen oxides (NO_x) [1]. The term NO_x refers to nitrogen monoxide (NO) along with nitrogen dioxide (NO_2) and those emissions have attracted special attention given to their environmental impact through ozone depletion, the formation of photochemical smog, acid rain or effects on human health. As the transport sector is the largest source of NO_x emissions (Fig. 1.1), the first legislation involving NO_x restrictions was introduced 1992 in Europe by the Euro I standard for light- and heavy-duty engines [2]. Since then, the establishment of standards for on-road vehicles were consecutively adjusted with increasingly stringent restrictions (Fig. 1.1). For the upcoming Euro VII proposal [3] in heavy-duty vehicles, a NO_x emission standard of no more than 0.35/0.09 g·kWh^{-1} (cold/hot emissions) is set. Further, limitations for nitrous oxide (N_2O) are considered, as N_2O is a strong greenhouse gas with a 300 times higher potential as CO_2 [4].

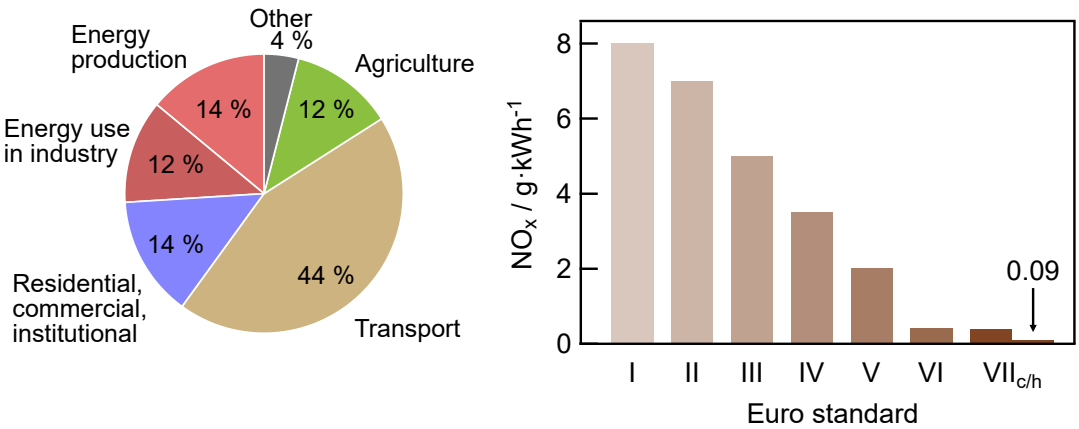

Figure 1.1: *NO_x emissions divided by source sector [5] and historical Euro emission standards of NO_x for heavy-duty vehicles. Data taken from [3, 6].*

Diesel engines are widespread in heavy-duty vehicles and the marine transport given to the beneficial economical operation and the higher thermodynamic

efficiency, making them irreplaceable to date [7]. Three-way catalysts perform well for gasoline engines, given that the time-average exhaust composition contains a stoichiometric 1:1 ration of oxidizing and reducing compounds to oxidize carbon monoxide as well as hydrocarbons and reduce NO_x gases [8]. In contrast, the diesel engines continuously operate in an oxidizing environment (lean conditions) with an excess of oxygen in the exhaust gas resulting in a unavoidable NO_x formation. A variety of techniques have been implemented to tackle this issue. The engine-out emissions were considerably lowered by reducing the nitrogen content in the fuel and an effective engine development such as improved engine design along with fuel injection equipment [9, 10]. However, the after treatment technology is considered to be the most suitable strategy to meet the emission standards and has initiated an entire research field in the diesel emission control starting from the 1980s. The most commonly used method is the selective catalytic reduction that utilizes ammonia as a reducing agent (NH_3-SCR) to convert NO_x gases selectively to N_2 and H_2O. Although, SCR systems originally were operated only in industrial plants since 1970 [11, 12], they are nowadays implemented in millions of mobile sources. From the very beginning, vanadium-based catalysts have been used catalysts as they have many advantages such as low material costs and a high resistance to sulfur compounds [12, 13]. In addition, the low N_2O formation is an important aspect considering the potential new emission standards for heavy-duty vehicles [3].

However, the implementation in mobile sources demands different requirements and the catalysts have to be optimized to achieve a high efficiency in a dynamic system that includes fluctuating temperatures and exhaust gas compositions. Thermal durability must be given to endure the vehicle lifetime and the increasing utilization of bio-fuel demands a firm resistance to the various combustion gases.

1.1 Objectives

The objective of this thesis is to achieve a scientific understanding of titania supported vanadium oxide catalysts for the NH_3-SCR reaction by using multiple *ex-situ* characterisation techniques and *in-situ* spectroscopic analysis methods. The focus is on understanding the effect of the vanadium loading and determination of the surface composition and changes after aging. The aging procedure was conducted by thermal treatment of the samples to simulate the long-term application. In addition, the promoting effect of Ce- and Nb-based additives in relation to the promoter interaction with TiO_2 as well as the VO_x species was studied using the same approach.

2 Background

2.1 Selective catalytic reduction with ammonia

The abatement of NO_x emissions can be categorized into three classes, which include pre-combustion, combustion and post-combustion modifications [9, 10]. The pre-combustion control can be achieved by lowering the nitrogen content in the fuel. In the combustion control, the emphasis lays on engine modifications such as an improved fuel delivery system and ignition timing. Although, the pre-combustion and combustion control are useful to reduce the NO_x formation, they only achieve a moderate reduction of NO_x emissions [14]. Nowadays, the emerged NO_x from the oxidation of organic nitrogen in the fuel is less considerable, due to the decrease of the nitrogen content in gasoline and diesel. The post-combustion control has turned out to an essential method to comply with the increasing stringent emission regulations, and focuses on reducing the NO_x gases after they have been formed in the combustion processes. The selective catalytic reduction with ammonia has been established as the leading technology to achieve this. In the SCR reaction, gaseous NO_x and ammonia are converted to harmless water and nitrogen. The main reactions in this process are the "Standard-SCR" and "Fast-SCR" reaction as described in Eq. 2.1 and 2.2.

$$4\,NO + 4\,NH_3 + O_2 \rightarrow 4\,N_2 + 6\,H_2O \tag{2.1}$$

$$NO + NO_2 + 2\,NH_3 \rightarrow 2\,N_2 + 3\,H_2O \tag{2.2}$$

This process was initially introduced in the 1970s in Japan for stationary exhaust after-treatment systems [11, 12] until 1985 employed in Europe [7]. For the application mobile sources, a urea solution ($CO(NH_2)_2$) is used as NH_3 source and injected into the combustion gas stream. In presence of water and heat, the urea is converted to ammonia and CO_2.

Several types of SCR catalysts are used including metal oxides, zeolites, alkaline-earth or rare-earth metals. Among these, the titania supported vanadium oxide catalyst (VO_x/TiO_2) is one of the most common SCR catalysts thanks to its various benefits.

2.2 Vanadium-based SCR catalysts

Titania supported vanadium oxide catalysts (VO_x) are among the most common catalysts to be utilized in urea-based SCR systems because of their high activity even for a low vanadium content (∼1–2 wt%). In addition, the material costs are relatively low in comparison to other systems and the good resistance to sulfuric compounds facilitates the operation with biofuels. Also, the low formation of nitrous oxide (N_2O) [13] makes vanadium-based catalyst beneficial in comparison to copper-zeolites in particular. Anatase TiO_2 is considered to be the most suitable support given to the high dispersion of the VO_x surface species [15], chemical robustness [16] and a good resistance to corrosive gases such as SO_2 and SO_3 [17, 18].

The vanadium content or rather loading plays a crucial role for the activity, selectivity and thermal stability of the catalyst. At a low vanadium loading, the vanadium oxide species are dispersed on the support in a monomeric VO_4 coordination with three bridging Ti-O-V bonds and a terminal vanadyl (V=O) bond. Increasing the vanadium loading leads to the formation of oligomeric and polymeric VO_4 species with bridging V-O-V bonds up to the theoretical maximum of the monolayer coverage. Polymeric vanadium oxide species have found to have the highest specific activity by shortening the regeneration of the redox sites that results in an overall lower energy barrier of the catalytic cycle [19]. For a vanadium loading higher than the monolayer coverage, crystalline V_2O_5 nanoparticles begin to form [13]. In general, a low vanadium loading is beneficial for the temperature stability as the VO_x species are finely dispersed [20]. A higher vanadium loading improves the low-temperature activity but decreases the thermal stability along with enhancing the SO_2 oxidation as well as N_2O formation [19].

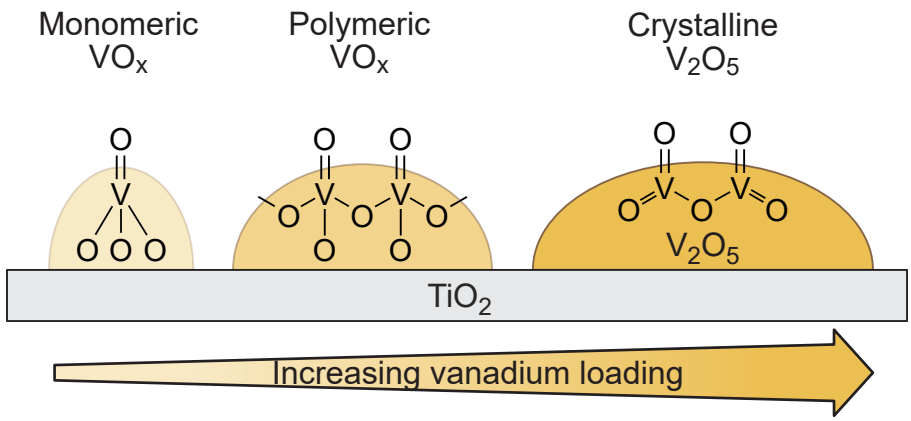

Figure 2.1: *Proposed structures of monomeric, polymeric and crystalline vanadium oxide species on the catalyst surface as a function of vanadium loading [13].*

2.2.1 Reaction mechanism and surface ammonia species

The formal oxidation state of supported vanadium oxide is either V^{5+} or V^{4+}, respectively oxidized V=O or hydrolyzed V-OH groups, which play a crucial role for the SCR reaction. Ammonia adsorbs on those sites either as surface NH_3 on a Lewis acid site or surface NH_4^+ on Brønsted acid site. Over the years, several reaction mechanisms based on two surface ammonia species have been proposed. The most commonly accepted reaction mechanism has been proposed by Topsøe et al. [21] in the early 1990s and contains both an acid and redox cycle. Ammonia adsorbs on the Brønsted acid site (Step 1) and is activated by an adjacent vanadium V=O site and reacts with gaseous or weakly adsorbed NO to form N_2 and H_2O (Step 2-3), while partially reducing the vanadium site. Lastly, the reduced site is regenerated by oxygen (Step 4). Based on this mechanism the formulation of a standard and fast SCR mechanism [22] and also the formulation of a mechanism over monomeric and polymeric vanadium species [19] have been elaborated. However, the exact nature of SCR reaction is still a subject of several investigations, as the importance of the Brønsted or Lewis acid sites is an ongoing debate [21, 23].

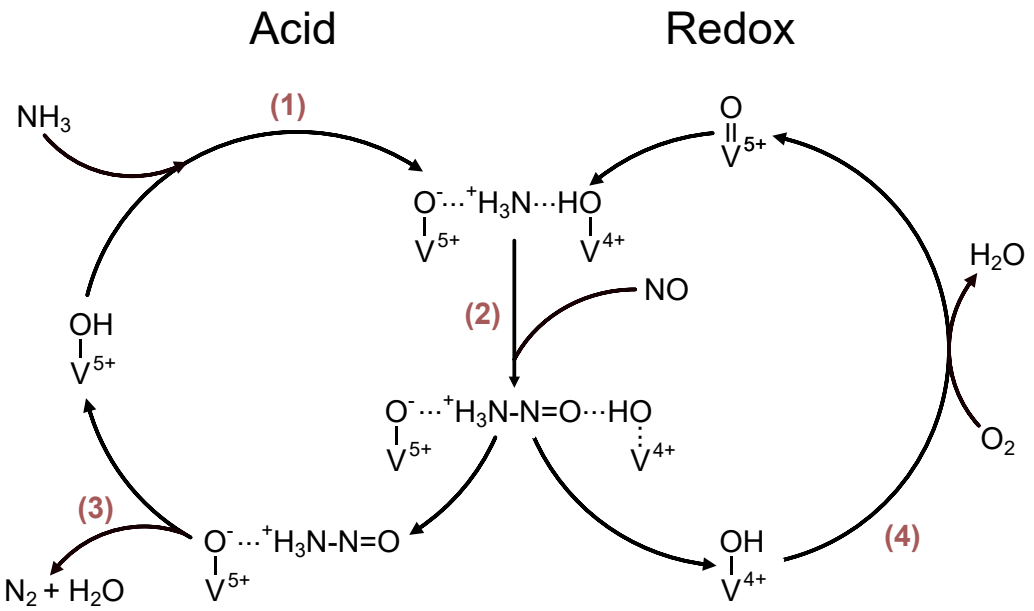

Figure 2.2: *Standard SCR mechanism proposed by Topsøe et al. [21]. The first step involves the ammonia adsorption (1) and activation by an adjacent V=O sites. The reaction with NO (2) leads to the formation of water and nitrogen (3) and the reduced sites is reoxidized (4).*

2.3 Challenges for V-based catalysts in mobile sources

The application in mobile sources demands several requirements. The SCR catalysts has to be highly efficient given to the limited available space in the exhaust gas treatment system and work under dynamic conditions. Depending on short distance driving in the city or long-range rides on the highway, the exhaust gas temperature can vary from 150 °C to 650 °C [20]. However, the high-efficiency operating window of vanadium-based catalysts is relatively narrow (∼300–400 °C), while exhaust temperatures can vary from 150 °C to 650 °C [20]. In addition, a lack of thermal stability is related to sintering of the VO_x particles forming crystalline V_2O_5 and unwanted side reactions occur at high temperatures. Another critical property is the vanadium volatility and release starting from 500 °C [24] causing incidental hazard risks to human health and the environment [25]. The Occupational Safety and Health Administration have declared V_2O_5 as a contaminant with strict disposal limits (0.5 mg/m^3 for dust) [26] and the U.S. Environmental Protection Agency have listed V_2O_5 as a harmful pollutant [27]. Therefore, the development of suitable SCR catalysts aims to stabilize the vanadium species along with setting the vanadium content as low as possible.

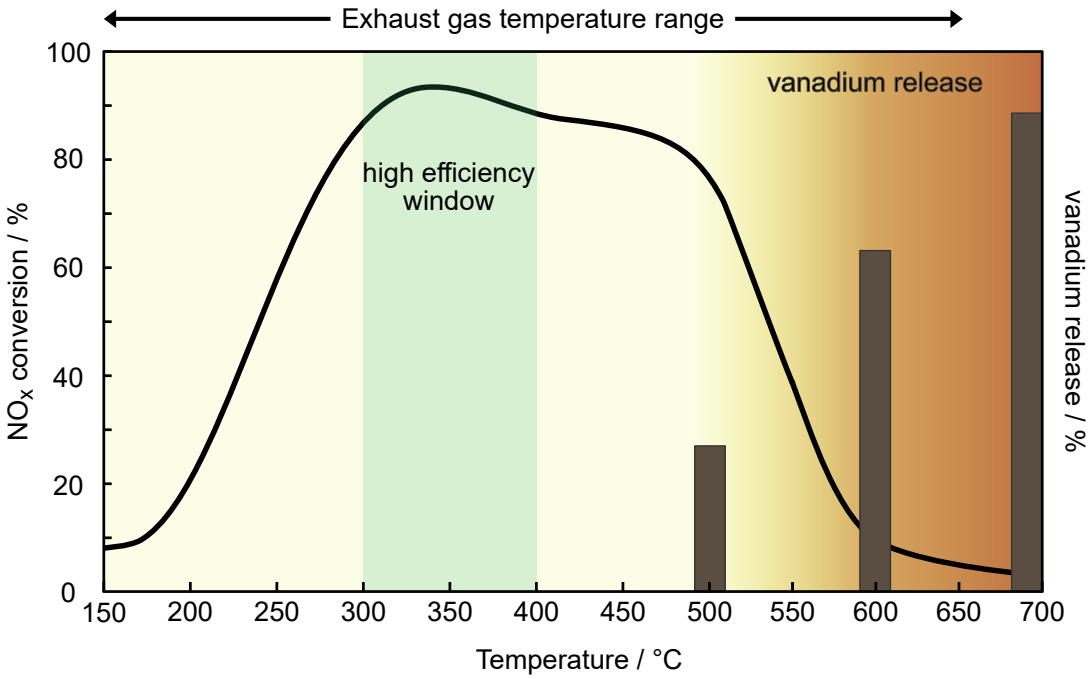

Figure 2.3: *Temperature operating window of a VO_x/TiO_2 catalyst: NO_x conversion versus temperature (left axis) and vanadium release (right axis). The data of the vanadium release is taken from [24].*

Therefore, both low-temperature activity as well as high-temperature stability must be given. Also, side reactions in the SCR process must be minimized including the SO_3 generation by SO_2 oxidation as well as further conversion to sulfuric acid (H_2SO_4) in the presence of moisture [13, 28, 29]. As mentioned in section 2.2, V-based catalysts are not thermally stable at temperatures starting from 500 °C [24]. The deactivation at high temperatures is both related to phase transformation from TiO_2 anatase to inactive TiO_2 rutile accompanied by a loss of surface area [30] and sintering of the VO_x particles. The formation of ammonium sulfate at low temperatures leads to a reduced catalytic activation due to the blocked surface of the catalyst and corrodes the post-treatment equipment [7]. Another important challenge is the unwanted site reaction of the nitrous oxide (N_2O) at high temperatures.

Summarizing, an ideal SCR catalyst should provide a broad temperature operating window with a high activity over the vehicle lifetime. A high low-temperature activity as well as stability at high temperatures up to ca. 650 °C is given. The potential risk of vanadium release to the atmosphere must be excluded or set to an absolute minimum. In addition, the catalyst should not be affected by any contaminants such as alkali metals or sulfuric compounds.

2.4 Implementation of promoters

In order to face the above-mentioned issues, the development for suitable SCR catalysts over the past couple of decades led to the implementation of various promoters based on W, Mo, Si, Mn, Ce, Nb, Sb and other elements [31]. Present industrial VO_x-SCR catalysts contain around 1-3 wt% vanadium to achieve a high ratio of polymeric VO_x and to minimize the undesired SO_2 oxidation.

Tungsten and molybdenum are the most widely promoters used and play a role in maintaining the structural and thermal stability of the VO_x species and enhance the resistance to sulfur. In particular, W extends the working temperature to a higher temperature range [32]. Silicon is proposed to be a valuable promoter for maintaining the stability of the TiO_2 support as it delays the sintering process [24, 33–36]. As the low-temperature activity is of major interest, promoters like cerium and manganese are used given to the high oxygen storage capacity and easy oxygen storage and release [37–40]. Because of the proprietary activity, catalysts based on manganese can be prepared without vanadium but often lack in resistance to water and SO_2. Niobium has found to increase the selectivity, surface acidity and resistance to SO_2 [41–43] as well as minimizing the formation of crystalline V_2O_5 phases [44]. When antimony is added in small amounts, it prevents catalyst poisoning by SO_2, and promotes the decomposition of ammonium bisulfate (ABS) [45–47]. Furthermore, Sb increases the redox ability of the catalyst surface beneficial for the low-temperature SCR reaction [43].

3 Methodology

A detailed description of the experimental procedures and characterization techniques used in this work is presented in this chapter. The catalytic activity of prepared samples was evaluated in a gas flow reactor. As the development for heterogeneous catalysts usually aims for a high surface area to give an extensive access for the reactants, the specific surface area (SSA) was determined by N_2-physisorption. The temperature programmed desorption of ammonia (NH_3-TPD) was used to evaluate the quantity and strength of the interaction between the catalyst surface and ammonia as main reactant. The formation of crystalline particles on the samples was investigated by X-ray diffraction (XRD). The spectroscopic investigation includes *in situ* DRIFT, Raman and X-ray photoelectron spectroscopy.

3.1 Sample preparation

The samples were prepared by incipient wetness impregnation of TiO_2 (DT-51D TiO_2, GfE GmbH). The impregnation solution was dissolved in a volume that corresponds the pore volume of the support. The promoted catalysts were prepared by co-impregnation of the promoter and vanadyl solution and added drop-wise to the support followed by subsequent mixing. The samples were calcined at 500 °C for 1 h. The resulting samples are labelled as fresh samples. For the thermal treatment, a portion of each fresh sample was heated at 550 °C for 100 h, referred to as aged samples.

The list of the applied chemicals for the preparation are presented in Table 3.1.

Table 3.1: *Chemicals used for the catalyst preparation and promoter solutions*

Name	Formula	Producer	Purity
DT51-D TiO_2	TiO_2	Tronox plc	99 wt% anatase
Vanadyl oxalate	$VO(C_2O_4)$	GfE GmbH	chemically pure
Cerium(III) nitrate	$Ce(NO_3)_3{\cdot}6H_2O$	Sigma-Aldrich	99.999%
Niobium(V) oxalate	$(NH_4)NbO(C_2O_4)_2$	Sigma-Aldrich	99.99%

3.2 Catalytic tests

The catalytic activity for the NO_x reduction over the pretreated samples was measured in a fixed-bed flow reactor under standard SCR conditions. The reaction conditions were set to simulate a realistic exhaust gas composition (500 ppm NO, 525 ppm NH_3, 300ppm CO, 3% CO_2, 10% O_2 and 5 vol% H_2O) in the temperature range of 175 to 450 °C. The effluent gas including NO, NH_3, NO_2 and N_2O was continuously analyzed and the NO_x conversion was calculated as follows:

$$\mathrm{NO_x\ conversion} = \frac{\mathrm{NO_{x,in}} - \mathrm{NO_{x,out}}}{\mathrm{NO_{x,in}}} \cdot 100\% \tag{3.1}$$

3.3 Characterization

3.3.1 Nitrogen physisorption

The physisorption with nitrogen is a method to measure the surface area of powder samples. Nitrogen is commonly used as gaseous adsorbate thanks to its high purity availability and the weak interaction with solids [48]. With the implementation of the Brunauer, Emmett and Teller (BET) method [49] the specific surface area (SSA) can be obtained. The BET theory follows the Langmuir theory on monolayer adsorption which correlates the partial pressure of the adsorbate and its adsorbed volume. The BET calculation includes the assumptions [50] (i) that the gas molecules behave ideally and adsorb on solids in layers infinitely, (ii) once adsorbed on the surface the gases are immobile and there is no adsorbate-adsorbate or interaction in between the layers, and (iii) the Langmuir theory can be applied to every layer. The resulting BET equation is expressed in Eq. 3.2.

$$\frac{P}{V(P_0 - P)} = \frac{C-1}{V_m C}\frac{P}{P_0} + \frac{1}{V_m C} \tag{3.2}$$

with P and P_0 as equilibrium and saturation pressure of the adsorbate, V is the total volume of adsorbed gas and C is the BET constant. At lower relative pressures (P/P_0<0.25) the behaviour follows a linear relationship and the nitrogen volume for monolayer formation (V_m) can be obtained from the slope or intercept of the regression line. With the given V_m, the SSA can be calculated in m^2/g (3.3).

$$\mathrm{SSA} = \frac{V_m \sigma N_A}{m V_{N_2}} \tag{3.3}$$

in which σ is the occupied area of a single N_2 molecule on the adsorbent, N_A the Avogadro constant, m as mass of investigated material and V_{N2} as the molar volume of N_2 at standard conditions.

In this work (**Paper I+II**), the specific surface area (SSA) was determined on all samples using a Micromeritics Tristar 3000 instrument, with degassing the samples in nitrogen prior to the measurements.

3.3.2 Temperature programmed desorption of ammonia

The experimental TPD procedure includes a pretreatment step at higher temperatures and an oxidizing or reducing atmosphere to remove any contaminants or gases on the surface. Then, the probe molecule is introduced at a low temperature until full saturation of the surface. After flushing with an inert gas to remove weakly adsorbed molecules, the temperature is slowly increased with a specific heating rate while the signal of the probing molecule is constantly recorded. As the temperatures increases, the adsorbates on different sites desorb and result in multiple sharp or broad desorption peaks [8]. In general, different peaks correspond to different surface sites. With a respective calibration, the integrated signal in a certain temperature interval can represent the concentration of a surface site.

In this work (**Paper I+II**), the TPD experiments were performed with ammonia (NH_3-TPD) as probing molecule to determine the NH_3 uptake of the support and catalysts.

3.3.3 Powder X-ray diffraction

The powder X-ray diffraction (XRD) is a conventional technique to evaluate crystallinity of a material. Further, it can provide information about the ratio of crystalline and amorphous compounds or the crystal structure, which can be pictured as a infinite plane of atoms in the crystal lattice. When X-rays interact with a crystalline material, the radiation is reflected when the scattered X-rays interfere constructively at specific angles. The X-ray wavelength (λ) is directly related to the spacing (d) between diffracting planes, as expressed in Bragg's law ($n{\cdot}\lambda = 2d{\cdot}\sin\theta$), where n represents any integer [51]. A schematic representation is displayed in Figure 3.1.

By scanning a range of incident angles, reflection occurs from planes that are oriented at the correct angle to fulfill the Bragg's Law [52]. The obtained XRD patterns imply characteristic fingerprints of atomic arrangements that can be compared with standard crystallographic databases for the qualitative analysis. Sharp and clear signals indicate a large crystals whereas broad peaks indicate smaller crystallites. The samples in both papers were analyzed by XRD to validate the formation of crystalline particles before and after the aging procedure. The diffraction patterns were collected with a Bruker AXS D8 instrument equipped with a Cu-Kα radiation source.

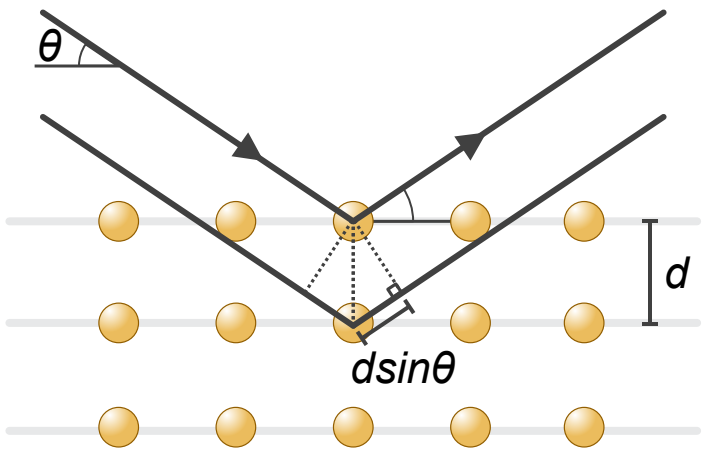

Figure 3.1: *Schematic representation of the Bragg's law with the reflection of X-rays by crystal planes. The distance (d) of the planes can be determined with the known X-ray wavelength (λ) and angle (θ).*

3.4 Spectroscopic techniques

Infrared (IR) spectroscopy is a useful method to probe compounds in solid, liquid or gaseous form. The method relies on the interaction of infrared photons with chemical compounds.

When IR radiation with equivalent energy is adsorbed, the vibrational or rotational modes of a covalent bond undergo a net change in the dipole moment. The various types of vibrations and rotations absorb at different frequencies within the infrared region and the energy transition depends on the mass of the respective atoms of the chemical bond as well as the bond strength. The bond strength can be affected by a range of factors like neighboring bonds, adsorption sites or temperature. Thus, unique spectral properties for the chemical bonds, functional groups or molecular species can be observed, which are sensitive in the adjacent environment [53]. Therefore, IR spectroscopy provides the possibility of identifying different compounds simultaneously as well as observing changes of the targeted species. The variation in absorbance at different wavenumbers gives rise to an absorption spectrum, which can be used for qualitative and quantitative analysis of the compound depending on the probing mode. The frequency of an absorption band is referred to as the wavenumber (cm^{-1}), and its energy is related to the strength of the bond and the atom mass at both ends. Figure 3.2 gives an example of a typical IR spectrum discussed in this thesis, where ammonia as a compound is adsorbed on a titania supported vanadium oxide catalyst. As the wavenumber of the vibration is sensitive to the adjacent environment of the chemical group/species under investigation, it is possible to obtain information

of the sites where the chemical group/species is adsorbed on, as shown in the chemical structures in Figure 3.2.

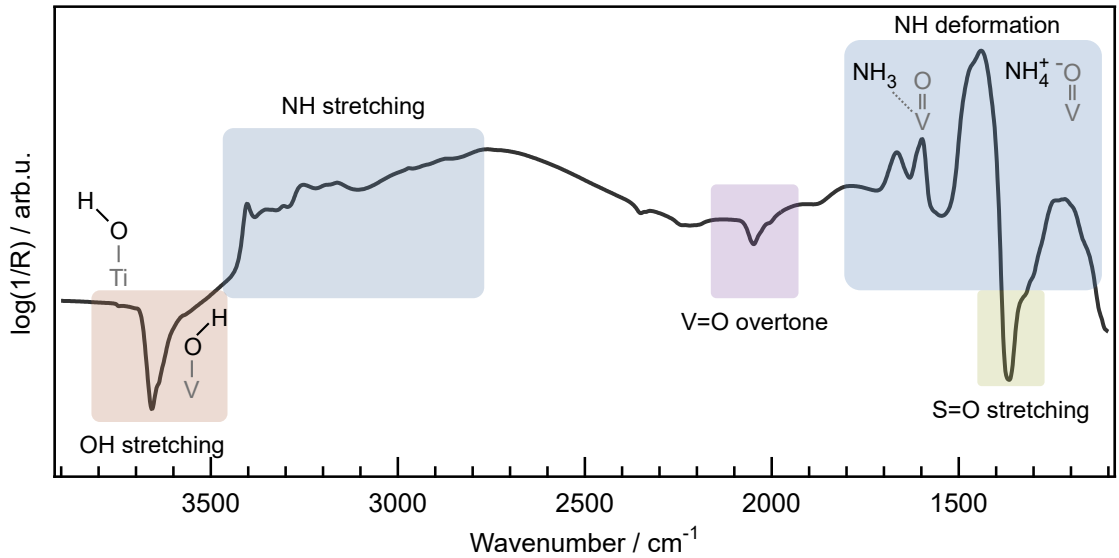

Figure 3.2: *Example of an IR spectrum (intensity vs. wavenumber) for the ammonia adsorption on a VO_x/TiO_2 catalyst. The marked regions represent the different vibration regions and examples of respective chemical groups.*

In this thesis, the mid-infrared region ranging from 900-4000 cm^{-1}, has been used for qualitative identification of surface-bound species on the investigated samples. An accurate molecular assignment of absorption bands requires a proper knowledge about vibrational modes. In general, an isolated non-linear molecule with N atoms has 3N-6 normal vibration modes (3N-5 for linear molecules). The product 3N corresponds to the three degrees of freedom including translation, rotation and vibration. As for example, ammonia has six (4·3-6) vibrational modes that are all IR active and correspond to symmetric and antisymmetric stretching as well as bending modes (Figure 3.3).

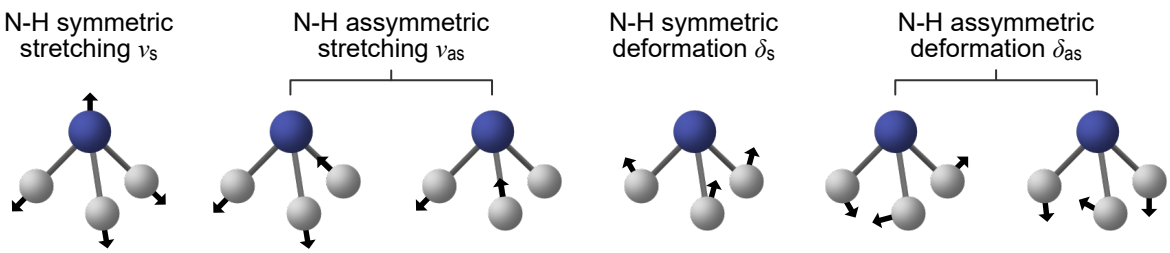

Figure 3.3: *Vibrational modes of isolated ammonia.*

3.4.1 In situ Diffuse Reflectance Infrared Fourier Transform Spectroscopy

Fourier transformed infrared spectroscopy in diffuse reflectance mode (DRIFTS) is common approach in the field of catalysis. Probe gas-phase reactants, product molecules as well as intermediate and spectator species adsorbed on the surface of the catalyst can be identified by their functional groups.

A simplified illustration of the DRIFTS set-up with emphasis on the sample cell is shown in Figure 3.8. Modulated infrared radiation is generated with a broadband light beam that goes through a Michelson interferometer (not shown in Figure 3.8) and is thereafter directed onto the powder sample. Upon hitting the rough surface of the sample it scatters within the sample (the scattering is limited by the penetration depth), interacts with the sample and is reflected in a diffuse manner in multiple angles. The reflected radiation is then collected and directed towards the detector [54]. The collected raw data is called an interferogram where the relative intensity as a function of position of the change of the optical path length. With the Fourier transformation, the spectral raw data is converted to an absorption spectrum with intensity versus wavenumber.

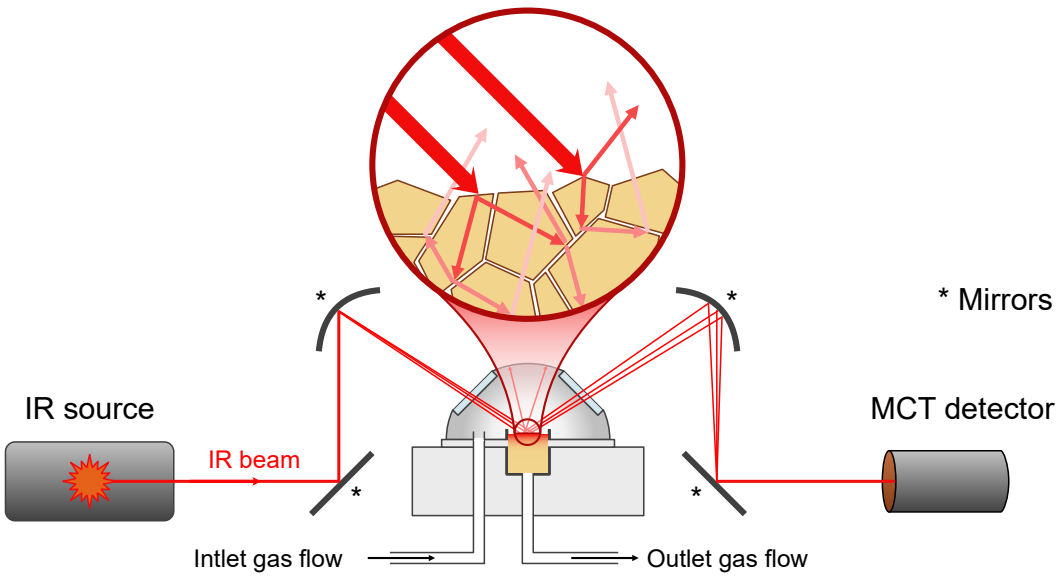

Figure 3.4: *Schematic illustration of an in situ diffuse reflectance infrared Fourier transformation setup: The IR beam is directed via mirrors onto the sample. The diffuse reflected radation is collected and guided to the MCT detector. The inlet gas flow and temperature can be controlled as required.*

Overall, the construction enables the rapid collection of an entire spectrum with a wide span of wavenumbers [55]. The DRIFTS technique is relatively simple to use as minimal sample preparation often only includes sieving the

powder sample to an appropriate particle size. A drawback is the lack of linear relationship between IR absorption and concentration of adsorbed species [56]. Hence, quantitative analysis requires many efforts and is commonly not considered. Instead, dynamic trends in the absorbance of different surface-bound species can be examined.

In this work, the qualitative investigation of surface species identification during NH_3/NO adsorption experiments have been carried out by *in situ* diffuse reflectance infrared Fourier transform spectroscopy (DRIFTS). A Bruker Vertex 70 spectrometer equipped with a high-temperature reaction cell (Harrick Scientific) with CaF_2 windows was used.

3.4.2 Peak profiles and deconvolution

Infrared spectra can result in a series of convoluted or overlapping vibration bands. As each molecule interacts differently with the surrounding and vibrate at different frequencies. In addition, certain compounds vibrate in a relatively narrow frequency window, which makes the assignment complicated and hinders the comparison of the relative amount.

Curve fitting or peak deconvolution is a helpful method to extract additional information from the spectra with the spectrum considered as the sum of individual peak profiles. For the choice of profiles, the natural relaxation and instrumental broadening must be considered. For solids, a low molecular movement is expected with a statistical distribution of environments that result in a Gaussian profile with a curving center and relatively narrow wings. For gases, a Lorentzian profile with broad wings is more convenient as frequent collisions as well as fast movements and rotations are considered. The Voigt profile is the convolution Gaussian and Lorentzian lines and is usually expressed for compounds in liquid state [57].

In this work, Voigt profiles have been used for the fitting the *in situ* DRIFT spectra, as the adsorbed gas or formed species are expected follow the Gaussian profile but further to include potential adsorbate-adsorbate interactions. These fittings were done on the NO adsorption spectra in **Paper I** and **II**.

3.4.3 Raman spectroscopy

Raman spectroscopy is based on elastic or inelastic scattering of infrared light to determine vibrational modes of a material. An intense and monochromatic laser (UV to near-infrared light) is used as excitation source to induce molecular vibrations or other excitations in the system, resulting in a shift in the frequency of the scattered light. This excitation results in a higher or lower vibrational state (Stokes, anti-Stokes scattering). An elastic scattering without energy change of the photon is the Rayleigh scattering. As at room temperature most of the

molecules are in ground vibrational state so that Stokes scattering has a higher probability than anti-Stokes. In general, Raman and infrared spectroscopy are used complementary as some vibrational modes cannot be observed in infrared, but are active in Raman and vice versa [58].

In this work (**Paper I+II**), Raman measurements were used for material characterization and the spectra were obtained with a InVia Reflex spectrometer from Renishaw with a 532 nm wavelength diode laser as excitation source using a laser power of 0.6 mW, to avoid any dehydration due to local heating. The optical image of selected spots was always checked before and after the measurements to ensure that no laser illumination damage occurred.

3.4.4 X-ray photoelectron spectroscopy

The X-ray photoelectron spectroscopy (XPS) is a surface sensitive method to obtain information about the surface composition, oxidation state and chemical environment of a species on the sample surface. The XPS method is based on the photoelectric effect, described by Albert Einstein [59], in which a photon is absorbed by an atom and induces the ejection of an electron (photoelectron) with a kinetic energy. The kinetic energy ($\mathrm{E_{kin}}$) of that ejected electron is described as the difference of the photon energy ($h\nu$) and binding energy of the electron ($\mathrm{E_b}$), as described in Equation 3.4.

$$\mathrm{E_{kin}} = h\nu - \mathrm{E_b} \tag{3.4}$$

The spectra are obtained by irradiating the surface with a beam of X-rays and measuring the number and kinetic energy of the ejected electrons from the top 1-10 nm of the material. The binding energies of the numerous photoelectrons emitted from a surface sample are used as a "fingerprint" to identify the present elements. The oxidation state can be determined by chemical shifts that are observed when an element enters a different bound state, which results in changes in the binding energy of core electrons.

4 Results and Discussion

This work is based on two studies that focus on the impact of the vanadium loading (**Paper I**) as well as the promoting effect of cerium and niobium (**Paper II**).

The respective vanadium loading is an important parameter for both activity and stability by reason of the formation of different VO_x surface species. According to previous studies [60–62], monomeric VO_x species are expected below a loading of 1.5 wt%, while crystalline V_2O_5 particles form at a loading higher than 4 wt%. Present industrial V-based catalysts contain around 2 wt% vanadium as a good compromise between activity and high temperature stability alongside with a high ratio of polymeric VO_x. In **Paper I**, a series of VO_x/TiO_2 model catalysts with five different vanadium loadings was prepared. Accordingly, this series is expected to include the entire range of VO_x species, with with only monomeric VO_x at a loading of 0.5 wt% and mainly crystalline V_2O_5 species at 8 wt%. The two samples with a loading of 1.5 and 4 wt% represent the transition zones with multiple VO_x species. As in automotive applications the thermal deactivation of the catalyst and potential volatility of vanadium is a major challenge, the the effect of thermal treatment, or aging respectively, was investigated on all samples.

The development of V-based NH_3-SCR catalysts led to the implementation of promoters like niobium or cerium as promising candidates in order to tackle the fore-mentioned challenges in mobile sources. In **Paper II**, the promoting effect of cerium and niobium were investigated by preparation of both promoted supports and model catalysts, with a respective vanadium loading of 2 wt%. The aim was to study the interaction of the promoters with the support and the vanadium species before and after aging.

4.1 Catalytic activity and correlation with physicochemical properties

4.1.1 Effect of vanadium loading

The catalytic activity of the prepared samples was evaluated by operation of the standard SCR reaction at temperatures between 170 to 450 °C (Fig. 4.1). In **Paper I**, the SCR activity tests revealed that a high vanadium loading is advantageous for high NO_x conversion over the fresh catalysts at lower temperatures, however low loadings suggest to be beneficial for the long-term application, as they maintain the activity after aging.

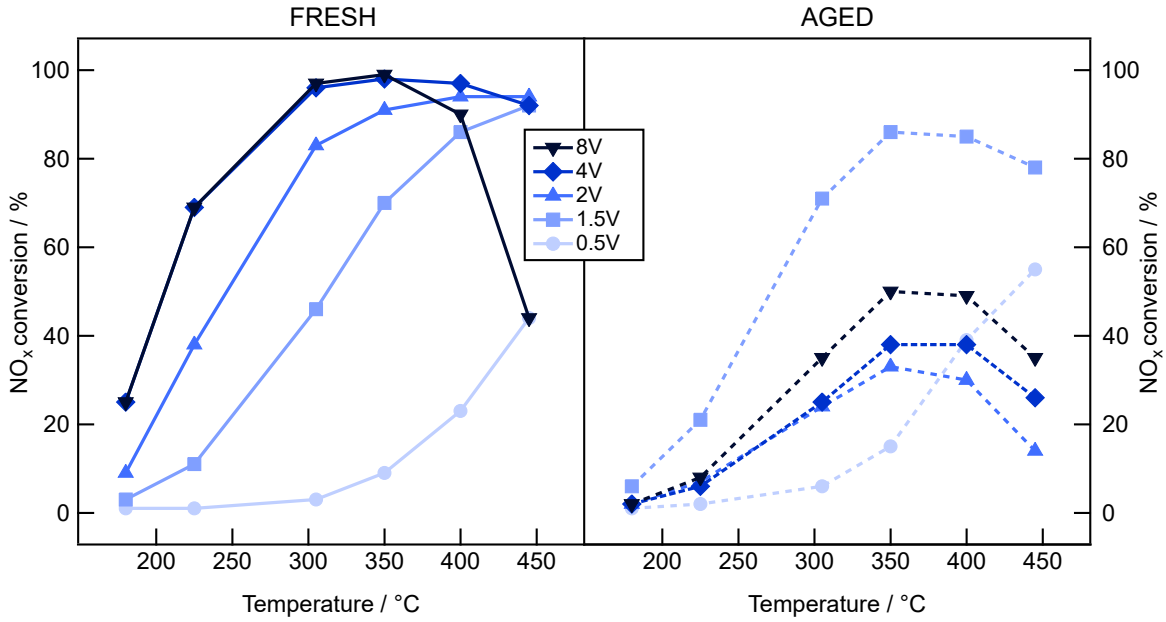

Figure 4.1: *NO_x conversion of the VO_x catalysts before and after aging. Reaction conditions: 525 ppm NH_3, 500 ppm NO, 300 ppm CO, 3% CO_2, 10% O_2, 5% H_2O in Ar/N_2 balance with a GHSV = 60.000 h^{-1}.*

As an example, the catalyst with a loading of 1.5 wt% shows a low NO_x conversion up to 220 °C (3-46%), moderate performance up to 350 °C and reaching the best performance of 92% at 450 °C. Yet, after the aging procedure the NO_x conversion is higher for low to mid-temperatures (180-350 °C), reaching its maximum of 86% at 350 °C, which indicates the formation of more polymerized VO_x species and increased activity. The conversion over the 8V catalyst achieves moderate conversions starting from 225 °C (69%) and reaching the overall highest NO_x conversion of 99% at 350 °C. However, the conversion drops significantly to 44% when reaching 450 °C, which is likely attributed to the partial oxidation of NH_3 to NO_x [63]. The overall lower NO_x conversions observed for the aged catalysts may also be related to VO_x sintering forming species that are less active

and/or V_2O_5 particles decreasing the number of accessible sites (vanadium atoms in "bulk")

Correlating the SSA measurements and the determined NH_3 uptake with the activity data suggests that those properties are not the limiting requirements or rather play a minor role for the SCR activity, in particular for the low temperature region. Given that the catalysts with a loading of 1.5 wt% still shows a decent activity after aging, despite losing more than about 60% of its SSA and 70% of NH_3 uptake. More likely the redox sites, hich are provided by vanadium [22, 64], seem to play a major role in the SCR reaction. Further, the decreasing values with increasing vanadium loading indicate that those parameters are mainly directed by the TiO_2 support showing an overall higher acidity than vanadium. The significant losses after aging mainly originate from TiO_2 particle growth [65] and sintering of the vanadium oxide particles that potentially lead to pore blocking [29, 30].

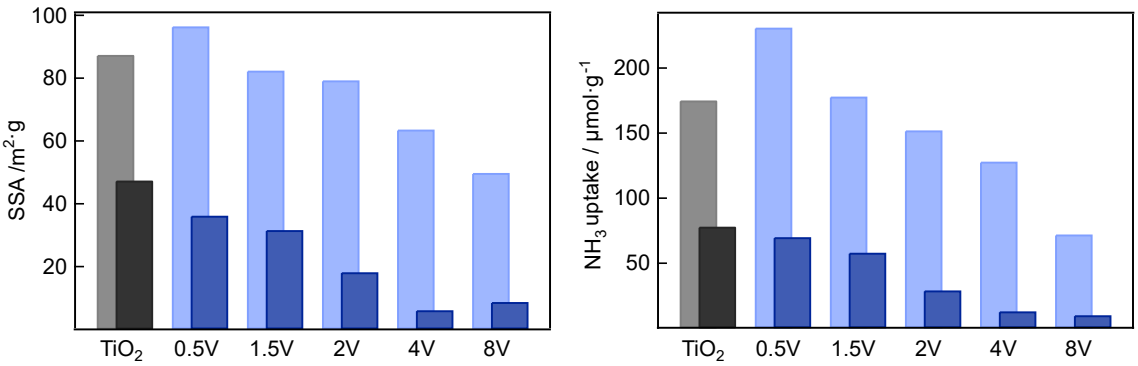

Figure 4.2: *Specific surface area (left) and determined NH_3 uptake (right) of the VO_x catalysts and TiO_2 before and after aging.*

4.1.2 Effect of promoters

For the investigation of the promoter effect in **Paper II**, the addition of cerium and niobium as promoters resulted in NO_x conversion rates that are similar to the of the reference VO_x/TiO_2 catalyst, with a slight advantage at lower temperatures (below 300 °C). For the Ce-promoted catalysts, the enhanced low-temperature activity can be attributed to the inherent redox capability of ceria [66]. The conversion over the aged catalysts revealed, that both catalysts maintained a high to moderate activity in comparison to the reference catalyst. However, the V-Ce/TiO_2 catalyst indicates to be more adversely affected, particularly at lower temperatures, where the conversion dropped significantly from 45% to 21% at 225 °C and notable decrease in the high-temperature region. On the other hand, the V-Nb/TiO_2 catalyst favours the preservation of the overall activity after aging, showing similar conversions up to 300 °C and just a slight decline of 4-7% at 350-400 °C.

The implementation of cerium and niobium demonstrated a notable preservation of the SSA than the catalyst reference after the aging procedure. While niobium indicates to have a higher stabilization effect by maintaining 51% of the SSA in comparison with V-Ce/TiO_2 (38%) and the reference catalyst (23%). The determined NH_3-uptake of both promoted catalysts is lower than for the reference catalyst, suggesting that both promoters do not contribute to the overall acidity. Nevertheless, it should be noted that the NH_3 uptake after aging are still considerably higher than for the reference catalyst.

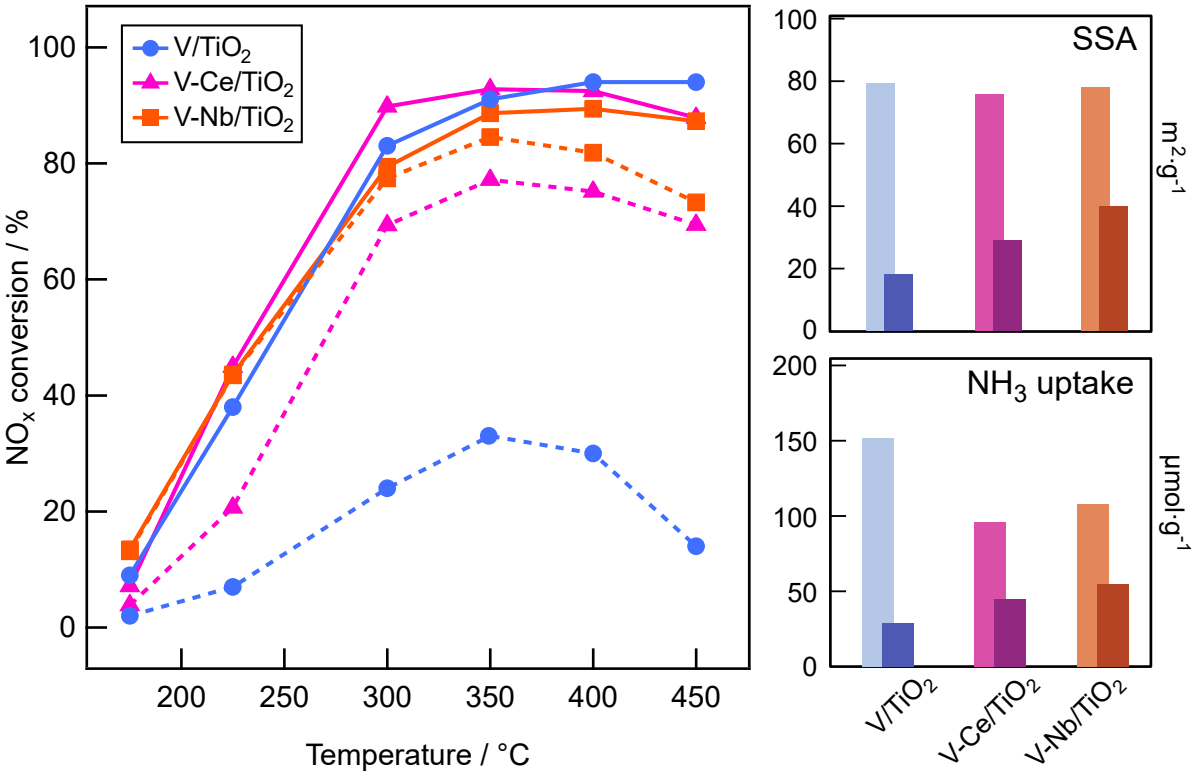

Figure 4.3: *NO_x conversion of the promoted VO_x catalysts before (solid lines) and after aging (dashed lines) as well results from SSA measurements and NH_3 uptake.*

4.2 Spectroscopic investigation of the catalyst surface

The secondary focus of this work was the investigation of the catalyst surface. Special emphasis was placed on the identification VO_x surface species and adsorbed species of the reactants.

In **Paper I**, Raman spectroscopy was used to identify the different VO_x species on the catalyst surface and respective transitions after the aging procedure

(Fig. 4.4). The Raman spectra recorded under ambient conditions exhibit predominantly features of the TiO_2 support at lower frequencies (396, 516, 638 cm^{-1}). These features gradually reduce as the vanadium loading increases, which is related to masking of vanadium of the support surface [18]. The existence of crystalline V_2O_5 is indicated by a sharp band at 995 cm^{-1} [18, 67, 68] and observed for the fresh catalysts starting from a vanadium loading of 4 wt% and thus confirming that the monolayer coverage is reached. After the aging procedure, crystalline V_2O_5 was even detected for the catalysts with a loading of 2 wt%. Polymeric VO_x species are commonly characterized by a band around 890 cm^{-1} that are related to V-O-V stretching vibrations [68], while the shoulder at 1019 cm^{-1} indicates a high degree of polymerization. The assignment for monomeric VO_x species is difficult given that the feature is only observed under dehydrated conditions. The remaining features in the range of 935-942 cm^{-1} have been assigned to V-O-Ti vibrations, considering the low vanadium amount on those samples. The observed mode shift with increasing loading could possibly indicate oligomerization or a higher degree of polymerized VO_x species.

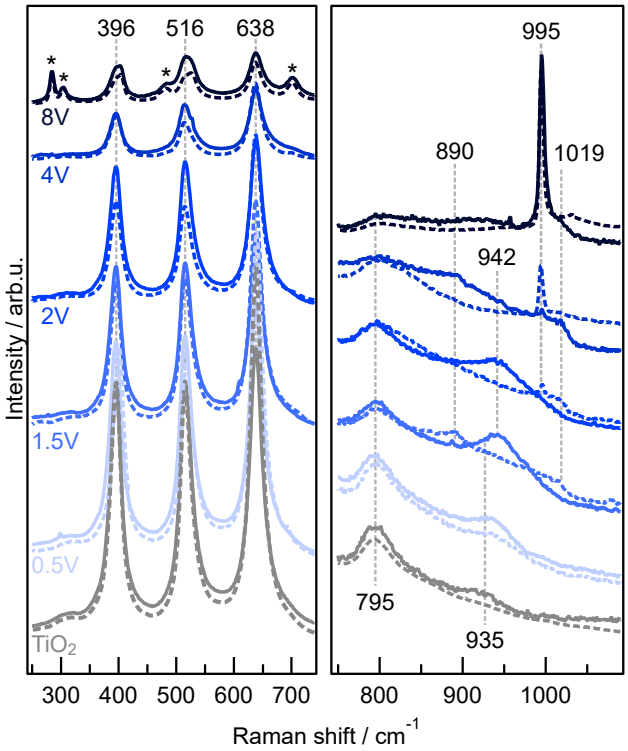

Figure 4.4: *Raman spectra of the VO_x catalysts and TiO_2 before (solid line) and after (dashed line) aging.*

DRIFT spectroscopy: NH_3 adsorption

In order to investigate the catalyst surface, it is fairly common to use suitable chemical probes that are IR active and adsorb on the surface. This interaction provides insights about the chemical properties of the surface and catalytic sites through their vibrational modes. Both NH_3 and NO are commonly used as probe molecules and their direct relevance for the NH_3-SCR reaction make them a special benefit in this work. For the surface characterization of the samples in this study, either NH_3 or NO adsorption experiments at room temperature were performed. It should be noted that these idealised conditions do not represent practical SCR reaction conditions, which involve additional components in the gas phase (water, oxygen, carbon dioxide etc.) and higher temperatures. In addition to that, the adsorption of NH_3 is temperature-dependent and Lewis-Brønsted site transformations can occur particularly in the presence of water [69, 70]. For this reason, the measurements at room temperature were performed for a qualitative comparison among the samples and provide an assignment of the species adsorbed on the surface.

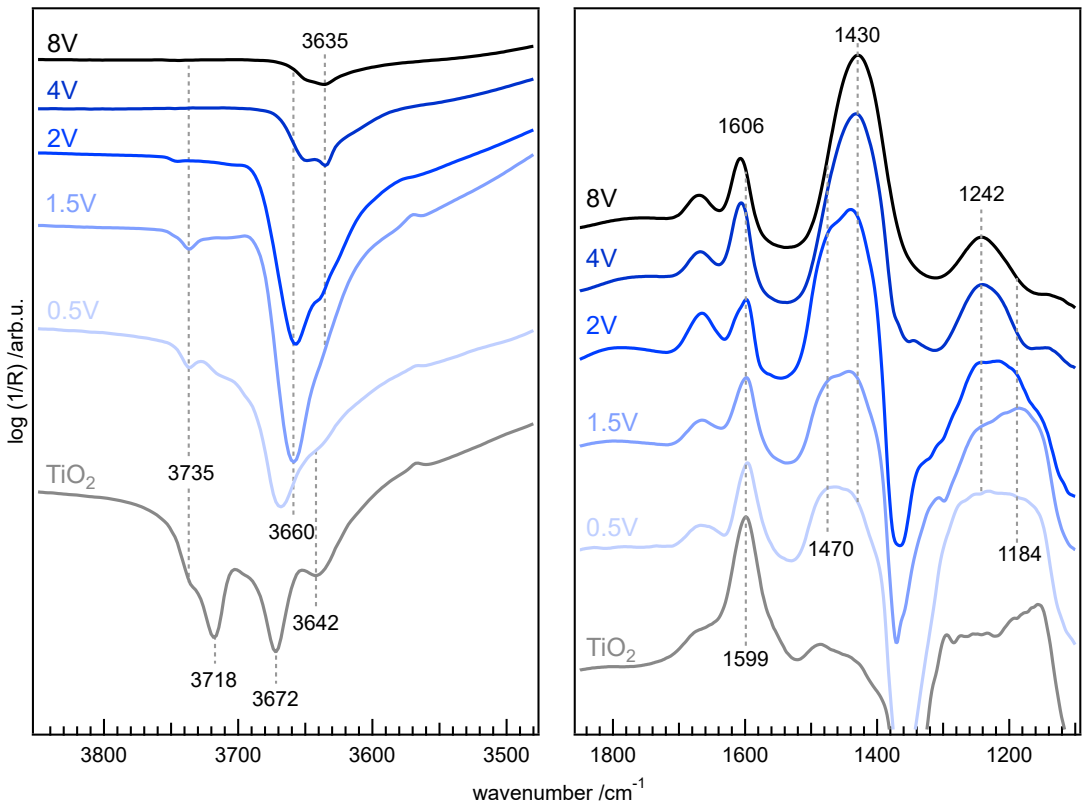

Figure 4.5: *DRIFT spectra for NH_3 at room temperature on the VO_x catalysts and TiO_2 support. ν(O-H) region (left) and δ(N-H) deformation modes (right) of NH_3 adsorbed on Lewis and Brønsted acid sites.*

To begin with the ammonia adsorption on the VO_x/TiO_2 samples (**Paper I**), there are two vibrational regions of interest. The N-H deformation region between 1800-1100 cm^{-1} allows the identification of coordinated NH_3 on Lewis acid sites alongside with NH_4^+ formed on Brønsted acid sites. Negative bands appear in the region between 3500 and 3800 cm^{-1} and provide information about the surface hydroxyl (OH) groups.

The O-H bands on the TiO_2 support are commonly related to isolated or terminal Ti-OH groups (3735, 3718 cm^{-1}) and bridged Ti-(OH)-Ti groups (3672, 3642 cm^{-1}) on different surface facets [65, 71]. With the introduction of vanadium, the isolated Ti-OH bands (3735, 3718 cm^{-1}) are significantly weaker, indicating that the vanadium oxides preferably interact with those groups and the new main band at 3660 cm^{-1} is related to isolated V-OH groups [69, 72]. When reaching a higher vanadium loading, an additional band at 3635 cm^{-1} can be identified and is assigned to bridged V-(OH)-V, following the analogy of the surface hydroxyl groups on TiO_2.

In the N-H deformation region, the characteristic δ_{as} band related to coordinately bonded NH_3 on Lewis acid sites are found around 1600 cm^{-1} as well as the respective split vibration at 1242-1150 cm^{-1} (δ_s). The δ_{as} band for NH_4^+ on Brønsted acid sites are found between 1470-1430 cm^{-1}. While the TiO_2 support mainly exhibits bands related to Lewis acid sites, the VO_x catalysts additionally reveal bands related to Brønsted acid sites. Throughout the sample series, two bands can be distinguished around 1470 and 1430 cm^{-1}, with the latter emerging as main band as the loading increases. According to the observations in the OH region, those bands are correlated to NH_4^+ formed on isolated V-OH and bridged V-(OH)-V or V-(OH)-Ti groups. In addition the shift of 1599 to 1606 cm^{-1} indicates a alternated environment given to the higher polymerization degree of the VO_x sites. The detailed outcomes of the band assignment for the ammonia adsorption are summarized in **Paper I**. After the aging procedure, the spectra general resulted in a reduced intensity of both O-H and N-H bands. In the O-H region the main band shifts to 3635 cm^{-1} indicating the oligomerization/polymerization of VO_x species to form bridged V-(OH)-V groups. In the N-H region, the δ_{as} vibration of Brønsted acid sites shifts to 1430 cm^{-1} as main signal.

Building upon the acquired knowledge, the band assignment was also conducted on the Nb- and Ce-promoted samples before and after aging in **Paper II**. In particular, by correlation of the OH signals from the promoted supports with those of the promoted catalysts, the differentiation of M-(OH), M-(OH)-V and M-(OH)-Ti was accomplished. Minor alterations in the adsorption spectra before and after aging suggests the stabilization impact of the promoters, consistent with the activity data.

DRIFT spectroscopy: NO adsorption

The NO adsorption was performed in order to describe the general chemical processes relevant for the reactive adsorption of NO on the samples at room temperature (Fig. 4.6). In general, the interaction of NO_x on catalysts is only partly understood. The assignment of the different species is difficult given to the large number of species coexisting on the surface and overlapping bands within a narrow wavenumber region. However, it is commonly accepted that mainly nitrates, NO and NO_2 are adsorbed on vanadium-titanium oxide surfaces [73, 74].

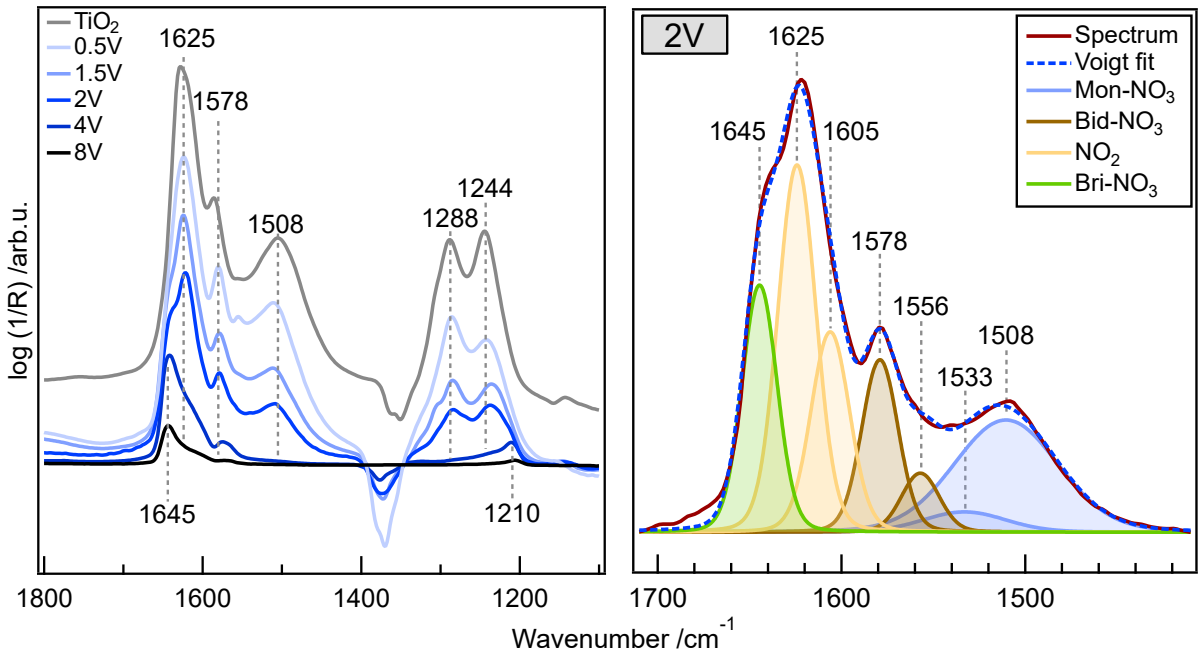

Figure 4.6: *DRIFT spectra for NO at room temperature on the prepared VO_x catalysts and TiO_2 support (left). Deconvoluted spectrum for the 2 wt% VO_x catalyst (right).*

The region of interest (1800 and 1100 cm^{-1}) is related to $\tilde{\nu}$(N=O) and $\tilde{\nu}_{as}$(ONO) vibrations of surface nitrates as well as gaseous or weakly adsorbed NO_2. Based on the values found in literature [74–76], the assignment of bridged nitrates (1645 cm^{-1}), bidentate (1578 cm^{-1}) and monodentate nitrates (1508 cm^{-1}) as well as their respective split vibrations was made. The main band for most of the samples is centered around 1625 cm^{-1} and is related to NO_2. With increasing vanadium loading the main band shifts to bridged nitrates (1645 cm^{-1}) as prevalent species. In order to investigate the relative ratio change of the respective species, the adsorption spectra were deconvoluted through fitting by Voigt profiles. The fitted peaks were integrated to give a comparison of the relative proportions of the different NO_x species on the samples. The peak deconvolution revealed additional bands for NO_2, bidentate and monodentate nitrates. A detailed band assignment of NO_x surface species on VO_x/TiO_2 along with the respective wavenumbers are summarized in **Paper I**.

Fig. 4.7 displays the relative integrated peak ratio of the NO_x surface species. For the bare TiO_2, adsorbed NO_2 and monodentate nitrates are the dominant species on TiO_2, followed by bidentate nitrates and bridged nitrates as smallest fraction. As the vanadium loading increases, the relative fraction of monodentate nitrates declines while the ratio of bridged nitrates steadily increases. Adsorbed NO_2 is the dominant species for most of the catalysts, as only the highest vanadium loading (8 wt%) reveals bridged nitrates as main species. These results indicate that bridged nitrates are preferably formed on crystalline V_2O_5 particles.

Based on the previous proficiency, the peak deconvolution was also conducted for the promoted catalysts as well as supports before and after aging (**Paper II**). The results from the integrated peak area show a different distribution of the surface NO_x species. In comparison with the bare support and the 2V catalysts, V-Ce/TiO_2 reveals a high ratio of bidentate nitrates, while V-Nb/TiO_2 exhibits a high ratio of bridged nitrates. Investigating whether those different distributions potentially link to the catalytic activity requires further studies under more dynamic conditions and also higher temperatures.

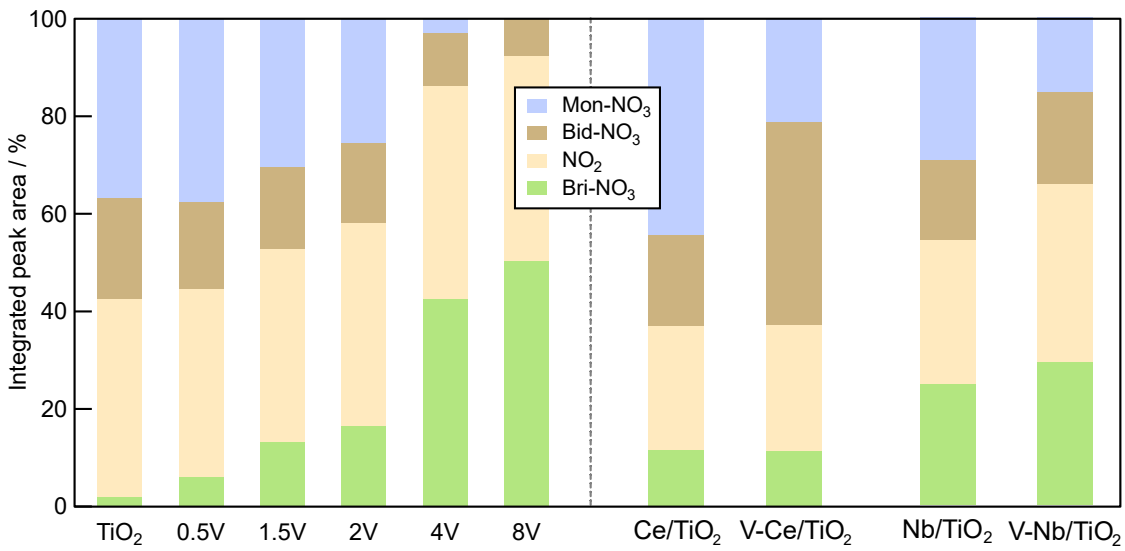

Figure 4.7: *Summary peak fitting: Relative ratio of NO_x species on TiO_2, VO_x catalysts and Nb/Ce-promoted samples.*

5 Conclusions and Future Work

The objective of this thesis the spectroscopic investigation of titania supported vanadium oxide catalysts in the NH_3-SCR reaction. This work aims to contribute to an overall improved fundamental understanding of VO_x-based catalysts for the application in mobile sources, guiding to a more rational catalyst design. The effect of the vanadium loading, implementation of two promoters (Ce, Nb) and aging impact were investigated by various ex-situ characterisation techniques, flow reactor measurements as well as spectroscopic methods.

In **Paper I**, the focus was to understand the effect of the vanadium loading and aging in terms of the catalytic performance and correlating the activity with the results obtained from *ex situ* characterization methods. A high vanadium loading reveals a high low-temperature activity in fresh state, whereas a low vanadium loading benefits to the thermal stability after aging. The results of the specific surface area (SSA) and NH_3-uptake indicate that those parameters are not the limiting requirements for the catalytic performance. Rather, the redox properties seem to play a major role in the SCR reaction. **Paper II** focused on the promoting effect of Ce- and Nb-based additives exploring the promoter interaction with TiO_2 and the VO_x species after aging. While the implementation of Ce promotes a higher low-temperature activity, the Nb incorporation favours a higher thermal stability. Nevertheless, both promoters contributed to an overall sustained activity after aging in comparison to the reference catalyst.

In situ DRIFTS experiments on the VO_x loading series (**Paper I**) allowed the assignment of surface hydroxyl (OH) groups as well as adsorbed (surface) species during the NH_3 and NO exposure. The deconvolution of NO_x adsorption peaks enabled the comparison of the ratio for the respective surface species. Based upon that knowledge, further band assignments have been conducted for the Ce- and Nb-promoted samples and the comparison of promoted support and catalysts allowed the identification of distinct OH surface sites and characteristics originating from the promoters in **Paper II**.

Based on the acquired knowledge on the surface species during the NH_3 and NO adsorption, future work will focus on the surface investigation under more dynamic conditions at elevated temperatures. Transient studies by pulsing gases can deliver insights into the differentiation of active or spectator species in the NH_3-SCR reaction. Further, the interaction of water on the catalyst surface and its impact during the reaction remains as an interesting research area. Future studies will focus on unraveling this effect and the modulation induced by promoters.

Acknowledgments

This work is financially supported by the Swedish Energy Agency through the FFI program "Ultra-efficient recyclable De-NO_x catalysts for biofuel and hybrid powertrains" (No. 51318-1) and the Competence Centre for Catalysis, which is hosted by Chalmers University of Technology and financially supported by the Swedish Energy Agency and the member companies AB Volvo, Johnson Matthey Plc, Perstorp AB, Powercell AB, Preem AB, Scania CV AB, Umicore AG & Co. KG.
The research presented in this thesis has been performed at the division of applied chemistry, competence centre for catalysis (KCK), and the Chalmers Material Analysis Laboratory, CMAL.

Further, I would like to thank:

- My supervisor Per-Anders Carlsson for the confidence and giving me the opportunity to work in this project. I am very grateful for your constant support and feedback throughout this time.
- My co-supervisor Anna Martinelli for the help with the Raman and writing feedback from an "outside" perspective.
- Andreas Schaefer for the support in various aspects ranging from practical and software-related matters as well as conducting the XPS measurements.
- Agnes Raj, Andrew Newman and Roberta Villamaina for the interest in my research and the constructive meetings.
- My examiner Magnus Skoglundh for evaluating my research progress and providing a motivating environment in the KCK. Lasse Urholm and Lennart Norberg for the help and maintenance of the KCK setups and equipment.
- Lotta Pettersson, Anna Oskarsson and Frida Andersson for the administrative work and organization of the various parties and events, making the TYK a great place to work.
- All the current and former members of my working group namely Chris, Felix, Guido, Mengqiao and Yanyue as well as all colleagues from TYK and KCK for the nice and pleasant atmosphere that includes the fika, after-works and much more.

References

[1] U.S.E.P. Agency, Clean air act requirements and history, http://www.epa.gov, Accessed: 2023-08-22.

[2] The European Commission, Council Directive 91/441/EEC amending Directive 70/220/EEC on the approximation of the laws of the Member States relating to measures to be taken against air pollution by emissions from motor vehicles, Brussels, **1991**-06-26. https://eur-lex.europa.eu/legal-content/EN/ALL/?uri=CELEX%3A31991L0441, Accessed: 2023-08-22.

[3] The European Commission, COM(2022) 586: Proposal for a regulation on type-approval of motor vehicles and engines and of systems, components and separate technical units intended for such vehicles, with respect to their emissions and battery durability (Euro 7), Brussels, **2022**-11-10. https://single-market-economy.ec.europa.eu/publications/euro-7-standard-proposal_en, Accessed: 2023-08-22.

[4] Zhu, M.; Lai, J. K.; Wachs, I. E. Formation of N_2O greenhouse gas during SCR of NO with V_2O_5 by supported vanadium oxide catalysts. *Applied Catalysis B: Environmental* **2018**, *224*, 836–840.

[5] European Energy Agency, European Union emission inventory report 1990-2020. *Under the UNECE Air Convention*, **2022**. https://www.eea.europa.eu/publications/european-union-emissions-inventory-report, Accessed: 2023-08-22.

[6] EU emission standards for heavy-duty CI (diesel) engines: Steady-state testing. In dieselnet.com. https://dieselnet.com/standards/eu/hd.php, Accessed: 2023-03-13.

[7] Nova, I.; Tronconi, E., *Urea-SCR Technology for deNO$_x$ After Treatment of Diesel Exhausts*; Springer, New York: **2014**, pp 3–31.

[8] Chorkendorff, I; Niemantsverdrie, J. In *Concepts of Modern Catalysis and Kinetics*; John Wiley & Sons, Ltd: **2003**; Chapter 4, pp 129–166.

[9] Cheng, X.; Bi, X. T. A review of recent advances in selective catalytic NO_x reduction reactor technologies. *Particuology* **2014**, *16*, 1–18.

[10] Skalska, K.; Miller, J. S.; Ledakowicz, S. Trends in NO_x abatement: A review. *Science of The Total Environment* **2010**, *408*, 3976–3989.

[11] Ando, J.; Tohata, H.; Isaacs, G. *NO_x Abatement for Stationary Sources in Japan*; U.S. Environmental Protection Agency, Cincinnati, Ohio, **1976**.

[12] Takagi, M.; Kawai, T.; Soma, M.; Onishi, T.; Tamaru, K. The mechanism of the reaction between NO_x and NH_3 on V_2O_5 in the presence of oxygen. *Journal of Catalysis* **1977**, *50*, 441–446.

[13] Lai, J. K.; Wachs, I. E. A Perspective on the Selective Catalytic Reduction (SCR) of NO with NH_3 by Supported V_2O_5-WO_3/TiO_2 Catalysts. *ACS Catalysis* **2018**, *8*, 6537–6551.

[14] Roy, S.; Hegde, M.; Madras, G. Catalysis for NO_x abatement. *Applied Energy* **2009**, *86*, 2283–2297.

[15] Busca, G.; Lietti, L.; Ramis, G.; Berti, F. Chemical and mechanistic aspects of the selective catalytic reduction of NO_x by ammonia over oxide catalysts: A review. *Applied Catalysis B: Environmental* **1998**, *18*, 1–36.

[16] Godiksen, A. L.; Rasmussen, S. B. Identifying the presence of $[V{=}O]^{2+}$ during SCR using in-situ Raman and UV Vis spectroscopy. *Catalysis Today* **2019**, *336*, 45–49.

[17] Lietti, L.; Alemany, J. L.; Forzatti, P.; Busca, G.; Ramis, G.; Giamello, E.; Bregani, F. Reactivity of V_2O_5-WO_3/TiO_2 catalysts in the selective catalytic reduction of nitric oxide by ammonia. *Catalysis Today* **1996**, *29*, 143–148.

[18] Vuurman, M. A.; Wachs, I. E.; Hirt, A. M. Structural determination of supported V_2O_5-WO_3/TiO_2 catalysts by in situ Raman spectroscopy and X-ray photoelectron spectroscopy. *Journal of Physical Chemistry* **1991**, *95*, 9928–9937.

[19] He, G.; Lian, Z.; Yu, Y.; Yang, Y.; Liu, K.; Shi, X.; Yan, Z.; Shan, W.; He, H. Polymeric vanadyl species determine the low-temperature activity of V-based catalysts for the SCR of NO_x with NH_3. *Science Advances* **2018**, *4*, 1–8.

[20] Madia, G.; Elsener, M.; Koebel, M.; Raimondi, F.; Wokaun, A. Thermal stability of vanadia-tungsta-titania catalysts in the SCR process. *Applied Catalysis B: Environmental* **2002**, *39*, 181–190.

[21] Topsøe, N. Y.; Dumesic, J. A.; Topsøe, H. Vanadia-titania catalysts for selective catalytic reduction of nitric-oxide by ammonia. II. Studies of active sites and formulation of catalytic cycles. *Journal of Catalysis* **1995**, *151*, 241–252.

[22] Arnarson, L.; Falsig, H.; Rasmussen, S. B.; Lauritsen, J. V.; Moses, P. G. A complete reaction mechanism for standard and fast selective catalytic reduction of nitrogen oxides on low coverage $VO_x/TiO_2(001)$ catalysts. *Journal of Catalysis* **2017**, *346*, 188–197.

[23] Marberger, A.; Ferri, D.; Elsener, M.; Kröcher, O. The Significance of Lewis Acid Sites for the Selective Catalytic Reduction of Nitric Oxide on Vanadium-Based Catalysts. *Angewandte Chemie - International Edition* **2016**, *55*, 11989–11994.

[24] Liu, Z. G.; Ottinger, N. A.; Cremeens, C. M. Vanadium and tungsten release from V-based selective catalytic reduction diesel aftertreatment. *Atmospheric Environment* **2015**, *104*, 154–161.

[25] Barceloux, D. G.; Barceloux, D. D. Vanadium. *Journal of Toxicology: Clinical Toxicology* **1999**, *37*, 265–278.

[26] Taylor, J.; Keith, S.; Cseh, L.; Ingerman, L.; Chappell, L.; Rhoades, J.; Hueber, A. *Toxicological profile for Vanadium*; U.S. Department of health and human services, Atlanta, **2012**.

[27] *U.S. EPA. IRIS Toxicological Review of Vanadium Pentoxide (External Review Draft, 2012)*; U.S. Environmental Protection Agency, Washington DC, **2011**.

[28] Jaegers, N. R.; Lai, J. K.; He, Y.; Walter, E.; Dixon, D. A.; Vasiliu, M.; Chen, Y.; Wang, C.; Hu, M. Y.; Mueller, K. T.; Wachs, I. E.; Wang, Y.; Hu, J. Z. Mechanism by which Tungsten Oxide Promotes the Activity of Supported V_2O_5/TiO_2 Catalysts for NO_x Abatement: Structural Effects Revealed by 51V MAS NMR Spectroscopy. *Angewandte Chemie - International Edition* **2019**, *58*, 12739–12746.

[29] Wachs, I. E. Catalysis science of supported vanadium oxide catalysts. **2013**, *42*, 11762–11769.

[30] Koebel, M.; Elsener, M.; Kleemann, M. Urea-SCR: a promising technique to reduce NO_x emissions from automotive diesel engines. *Catalysis Today* **2000**, *59*, 335–345.

[31] Chen, C.; Cao, Y.; Liu, S.; Chen, J.; Jia, W. Review on the latest developments in modified vanadium-titanium-based SCR catalysts. *Chinese Journal of Catalysis* **2018**, *39*, 1347–1365.

[32] Lietti, L.; Nova, I.; Ramis, G.; Dall'Acqua, L.; Busca, G.; Giamello, E.; Forzatti, P.; Bregani, F. Characterization and Reactivity of V_2O_5–MoO_3/TiO_2 De-NO_x SCR Catalysts. *Journal of Catalysis* **1999**, *187*, 419–435.

[33] Chapman, D. M.; Fu, G.; Augustine, S.; Watson, M.; Crouse, J.; Zavalij, L.; Perkins-Banks, D. New Titania Materials with Improved Stability and Activity for Vanadia-Based Selective Catalytic Reduction of NO_x. *SAE International Journal of Fuels and Lubricants* **2010**, *3*, 643–653.

[34] Kobayashi, M.; Kuma, R.; Masaki, S.; Sugishima, N. TiO_2-SiO_2 and V_2O_5/TiO_2-SiO_2 catalyst: Physico-chemical characteristics and catalytic behavior in selective catalytic reduction of NO by V_2O_5. *Applied Catalysis B: Environmental* **2005**, *60*, 173–179.

[35] Pan, Y.; Zhao, W.; Zhong, Q.; Cai, W.; Li, H. Promotional effect of Si-doped V_2O_5/TiO_2 for selective catalytic reduction of NO_x by V_2O_5. *Journal of Environmental Sciences* **2013**, *25*, 1703–1711.

[36] Beale, A. M.; Lezcano-Gonzalez, I.; Maunula, T.; Palgrave, R. G. Development and characterization of thermally stable supported V–W–TiO_2 catalysts for mobile V_2O_5–SCR applications. *Catalysis, Structure and Reactivity* **2015**, *1*, 25–34.

[37] Wu, Z.; Jin, R.; Wang, H.; Liu, Y. Effect of ceria doping on SO_2 resistance of Mn/TiO_2 for selective catalytic reduction of NO with V_2O_5 at low temperature. *Catalysis Communications* **2009**, *10*, 935–939.

[38] Zhang, S.; Zhang, B.; Liu, B.; Sun, S. A review of Mn-containing oxide catalysts for low temperature selective catalytic reduction of NO_x with NH_3: reaction mechanism and catalyst deactivation. *RSC Adv.* **2017**, *7*, 26226–26242.

[39] Liu, Z.; Zhang, S.; Li, J.; Zhu, J.; Ma, L. Novel V_2O_5-CeO_2/TiO_2 catalyst with low vanadium loading for the selective catalytic reduction of NO_x by NH_3. *Applied Catalysis B: Environmental* **2014**, *158-159*, 11–19.

[40] Zhang, Y.; Zhu, X.; Shen, K.; Xu, H.; Sun, K.; Zhou, C. Influence of ceria modification on the properties of TiO_2-ZrO_2 supported V_2O_5 catalysts for selective catalytic reduction of NO by NH_3. *Journal of Colloid and Interface Science* **2012**, *376*, 233–238.

[41] Lian, Z.; Liu, F.; He, H.; Liu, K. Nb-doped VO_x/CeO_2 catalyst for NH_3-SCR of NO_x at low temperatures. *RSC Advances* **2015**, *5*, 37675–37681.

[42] Lian, Z.; Liu, F.; Shan, W.; He, H. Improvement of Nb Doping on SO_2 Resistance of VO_x/CeO_2 Catalyst for the Selective Catalytic Reduction of NO_x with NH_3. *Journal of Physical Chemistry C* **2017**, *121*, 7803–7809.

[43] Du, X.; Gao, X.; Fu, Y.; Gao, F.; Luo, Z.; Cen, K. The co-effect of Sb and Nb on the SCR performance of the V_2O_5/TiO_2 catalyst. *Journal of Colloid and Interface Science* **2012**, *368*, 406–412.

[44] Elbadawi, A. A. H.; Osman, M. S.; Razzak, S. A.; Hossain, M. M. VO_x-Nb/La-γAl_2O_3 catalysts for oxidative dehydrogenation of ethane to ethylene. *Journal of the Taiwan Institute of Chemical Engineers* **2016**, *61*, 106–116.

[45] Ye, D.; Qu, R.; Zheng, C.; Cen, K.; Gao, X. Mechanistic investigation of enhanced reactivity of NH_4HSO_4 and NO on Nb- and Sb-doped VW/Ti SCR catalysts. *Applied Catalysis A: General* **2018**, *549*, 310–319.

[46] Kwon, D. W.; Kim, D. H.; Lee, S.; Kim, J.; Ha, H. P. A dual catalytic strategy by the nature of the functionalization effect as well as active species on vanadium-based catalyst for enhanced low temperature SCR. *Applied Catalysis B: Environmental* **2021**, *289*, 120032.

[47] Kumar, P. A.; Jeong, Y. E.; Ha, H. P. Low temperature NH_3-SCR activity enhancement of antimony promoted vanadia-ceria catalyst. *Catalysis Today* **2017**, *293-294*, 61–72.

[48] Thommes, M.; Kaneko, K.; Neimark, A. V.; Olivier, J. P.; Rodriguez-Reinoso, F.; Rouquerol, J.; Sing, K. S. Physisorption of gases, with special reference to the evaluation of surface area and pore size distribution (IUPAC Technical Report). *Pure and Applied Chemistry* **2015**, *87*, 1051–1069.

[49] Brunauer, S.; Emmett, P. H.; Teller, E. Adsorption of Gases in Multimolecular Layers. *Journal of the American Chemical Society* **1938**, *60*, 309–319.

[50] Lowell, S.; Shields, J. E.; Thomas, M. A.; Thommes, M. In *Characterization of Porous Solids and Powders: Surface Area, Pore Size and Density*; Springer Netherlands: Dordrecht, **2004**, pp 129–156.

[51] Bragg, W. H.; Bragg, W. L. The reflection of X-rays by crystals. *Proceedings of the Royal Society of London. Series A, Containing Papers of a Mathematical and Physical Character* **1913**, *88*, 428–438.

[52] L.E Smart, E. M., *Solid State Chemistry: An Introduction, Fourth Edition (4th ed.).* CRC Press.: **2012**.

[53] H. Grünzler, H. G., *IR Spectroscopy: An Introduction*; WILEY-VCH: **2002**.

[54] Khoshhesab, Z. M., *Reflectance IR Spectroscopy*; Intech: **2012**.

[55] Harris, D., *Quantitative Chemical Analysis*; W. H. Freeman and Company, New York: **2010**.

[56] Sirita, J.; Phanichphant, S.; Meunier, F. C. Quantitative analysis of adsorbate concentrations by diffuse reflectance FT-IR. *Analytical chemistry* **2007**, *79*, 3912–3918.

[57] Bradley, M. *Curve Fitting in Raman and IR Spectroscopy: Basic Theory of Line Shapes and Applications*; **2007**.

[58] Larkin, P. In *Infrared and Raman Spectroscopy*; Elsevier: Oxford, **2011**.

[59] Einstein, A. *Annals of Physics* **1905**, *17*, 132.

[60] Went, G. T.; Leu, L. J.; Rosin, R. R.; Bell, A. T. The effects of structure on the catalytic activity and selectivity of V_2O_5/TiO_2 for the reduction of NO by NH_3. *Journal of Catalysis* **1992**, *134*, 492–505.

[61] Won, J. M.; Kim, M. S.; Hong, S. C. The cause of deactivation of VO_x/TiO_2 catalyst by thermal effect and the role of tungsten addition. *Chemical Engineering Science* **2021**, *229*, 116068.

[62] Ganjkhanlou, Y.; Janssens, T. V.; Vennestrøm, P. N.; Mino, L.; Paganini, M. C.; Signorile, M.; Bordiga, S.; Berlier, G. Location and activity of VO_x species on TiO_2 particles for NH_3-SCR catalysis. *Applied Catalysis B: Environmental* **2020**, *278*, 119377.

[63] Burkardt, D. A.; Weisweiler, W.; can den Tillaart, J.; Schäfer-Sindlinger, A.; Lox, E. Influence of the V_2O_5 Loading on the Structure and Activity of V_2O_5/TiO_2 SCR Catalysts for Vehicle Application. *Topics in Catalysis* **2001**, *16*, 369–375.

[64] Marberger, A.; Elsener, M.; Ferri, D.; Kröcher, O. VO_x surface coverage optimization of V_2O_5/WO_3-TiO_2 SCR catalysts by variation of the V loading and by aging. *Catalysts* **2015**, *5*, 1704–1720.

[65] Kubacka, A.; Iglesias-Juez, A.; di Michiel, M.; Becerro, A. I.; Fernández-García, M. Morphological and structural behavior of TiO_2 nanoparticles in the presence of WO_3: Crystallization of the oxide composite system. *Physical Chemistry Chemical Physics* **2014**, *16*, 19540–19549.

[66] Tang, C.; Zhang, H.; Dong, L. Ceria-based catalysts for low-temperature selective catalytic reduction of NO with NH_3. *Catalysis Science and Technology* **2016**, *6*, 1248–1264.

[67] Machej, T.; Haber, J.; M. Turek, A.; E. Wachs, I. Monolayer V_2O_5/TiO_2 and MoO_3/TiO_2 catalysts prepared by different methods. *Applied Catalysis* **1991**, *70*, 115–128.

[68] Went, G. T.; Leu, L.-J.; Bell, A. T. Quantitative structural analysis of dispersed vanadia species in TiO_2(anatase)-supported V_2O_5. *Journal of Catalysis* **1992**, *134*, 479–491.

[69] Ramis, G.; Busca, G.; Bregani, F.; Forzatti, P. Fourier transform-infrared study of the adsorption and coadsorption of nitric oxide, nitrogen dioxide and ammonia on vanadia-titania and mechanism of selective catalytic reduction. *Applied Catalysis* **1990**, *64*, 259–278.

[70] Topsøe, N. Y.; Slabiak, T.; Clausen, B. S.; Srnak, T. Z.; Dumesic, J. A. Influence of water on the reactivity of vanadia/titania for catalytic reduction of NO_x. *Journal of Catalysis* **1992**, *134*, 742–746.

[71] Fernández-García, M.; Belver, C.; Hanson, J. C.; Wang, X.; Rodriguez, J. A. Anatase-TiO_2 nanomaterials: Analysis of key parameters controlling crystallization. *Journal of the American Chemical Society* **2007**, *129*, 13604–13612.

[72] Busca, G.; Marchetti, L.; Centi, G.; Trifirò, F. Surface characterization of a grafted vanadium-titanium dioxide catalyst. *Journal of the Chemical Society, Faraday Transactions 1: Physical Chemistry in Condensed Phases* **1985**, *81*, 1003–1014.

[73] Hadjiivanov, K. I. Identification of neutral and charged N_xO_y surface species by IR spectroscopy. *Catalysis Reviews - Science and Engineering* **2000**, *42*, 71–144.

[74] Azambre, B.; Zenboury, L.; Koch, A.; Weber, J. V. Adsorption and desorption of NO_x on commercial ceria-zirconia ($Ce_xZr_{1-x}O_2$) mixed oxides: A combined TGA, TPD-MS, and DRIFTS study. *Journal of Physical Chemistry C* **2009**, *113*, 13287–13299.

[75] Hadjiivanov, K.; Bushev, V.; Kantcheva, M.; Klissurski, D. Infrared Spectroscopy Study of the Species Arising during NO_2 Adsorption on TiO_2 (Anatase). *Langmuir* **1994**, *10*, 464–471.

[76] Hadjiivanov, K.; Knözinger, H. Species formed after NO adsorption and NO + O_2 co-adsorption on TiO_2: An FTIR spectroscopic study. *Physical Chemistry Chemical Physics* **2000**, *2*, 2803–2806.